ChemPubSoc Europe

DOI: 10.1002/chem.201405442

CHEMISTRY
A European Journal
Full Paper

Enzyme Mimics | *Hot Paper*

Halogen Bonding Controls the Regioselectivity of the Deiodination of Thyroid Hormones and their Sulfate Analogues

Debasish Manna, Santanu Mondal, and Govindasamy Mugesh*[a]

Abstract: The type 1 iodothyronine deiodinase (1D-1) in liver and kidney converts the L-thyroxine (**T4**), a prohormone, by outer-ring (5′) deiodination to biologically active 3,3′,5-triiodothyronine (**T3**) or by inner-ring (5) deiodination to inactive 3,3′,5′-triiodothronine (**rT3**). Sulfate conjugation is an important step in the irreversible inactivation of thyroid hormones. While sulfate conjugation of the phenolic hydroxyl group stimulates the 5-deiodination of **T4** and **T3**, it blocks the 5′-deiodination of **T4**. We show that thyroxine sulfate (**T4S**) undergoes faster deiodination as compared to the parent thyroid hormone **T4** by synthetic selenium compounds. It is also shown that ID-3 mimics, which are remarkably selective to the inner-ring deiodination of **T4** and **T3**, changes the selectivity completely when **T4S** is used as a substrate. From the theoretical investigations, it is observed that the strength of halogen bonding increases upon sulfate conjugation, which leads to a change in the regioselectivity of ID-3 mimics towards the deiodination of **T4S**. It has been shown that these mimics perform both the 5′- and 5-ring deiodinations by an identical mechanism.

Introduction

Iodothyronine deiodinases (IDs) are mammalian selenoenzymes that play an important role in the thyroid hormone homeostasis.[1] Type 1 deiodinase (ID-1) can catalyse both the phenolic ring (5′) and tyrosyl ring (5) deiodination of prohormone 3,3′,5,5′-tetraiodothyronine (**T4**) to produce biologically active 3,3′,5-triiodothyronine (**T3**) and biologically inactive 3,3′,5′-triiodothyronine (**rT3**), respectively. In contrast, type 2 deiodinase (ID-2) and type 3 deiodinase (ID-3) mediates specific 5′- and 5-deiodination of **T4** to produce **T3** and **rT3**, respectively. Subsequent deiodination of **T3** and **rT3** by all three types of deiodinases produces biologically inactive metabolite **3,3′-T2** as shown in Scheme 1.[2] Apart from the enzymatic deiodination, sulfation of the 4′-hydroxyl group has been shown to be a major metabolic pathway of thyroid hormones. In general, sulfate conjugation is a natural detoxification mechanism to increase the water solubility of a variety of endogenous and exogenous lipophilic compounds and to facilitate their excretion in bile and/or urine.[3] However, sulfated thyroid hormones show very low affinity towards the thyroid hormone receptors, which indicates that the sulfation of thyroid hormones is an inactivation pathway. Cytosolic sulfotransferases (SULTs), which use 3′-phosphoadenosine-5′-phosphosulfate (PAPS) as a sulfate donor, catalyze the sulfate conjugation. Sulfotransferases, located in different tissues, such as liver, kidney, and brain, exist as homodimers with a molecular weight of 33 kDa.[4] Depending on the amino acid sequence and substrate specificity, SULTs are classified into four different subfamilies, such as SULT1, SULT2, SULT3 and SULT4. Among them only the SULT1 catalyzes the sulfate conjugation of iodothyronines.[3a,5] Isoforms of SULT1 show different affinity and substrate specificity towards thyroid hormones.

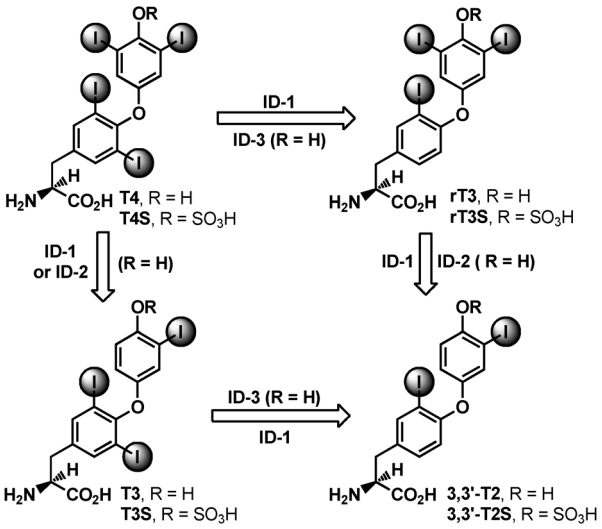

Scheme 1. Regioselective deiodinations of thyroid hormones and their sulfate analogues by iodothyronine deiodinases.

Similarly to the enzymatic deiodination of thyroid hormones, iodothyronine sulfates (**T4S**, **T3S**, **rT3S**, **3,3′-T2S**) also undergo deiodination by different deiodinases (Scheme 1).[6] Surprisingly, while the 5-deiodination of **T4S** by rat ID-1 is enhanced by

[a] *Dr. D. Manna, S. Mondal, Prof. Dr. G. Mugesh*
Department of Inorganic and Physical Chemistry
Indian Institute of Science
Bangalore 560012 (India)
E-mail: mugesh@ipc.iisc.ernet.in
Homepage: http://ipc.iisc.ernet.in/~mugesh/

Supporting information for this article is available on the WWW under http://dx.doi.org/10.1002/chem.201405442.

~200 fold relative to that of **T4**, ID-1 does not catalyse the 5′-deiodination of **T4S**.[7] Similarly, the sulfate conjugation has been shown to enhance the 5-deiodination of **T3S** (~40-fold) and 3′-deiodination of **3,3′-T2S** by rat and human ID-1.[7] In contrast, ID-2 and ID-3 do not accept T4S and/or T3S as substrates. Although the sulfate-conjugates of thyroid hormones undergo faster deiodination by IDs, the mechanism by which sulfate conjugation enhances the deiodination remains unknown.

In earlier reports, our group has shown that **1** and **2** bearing a thiol/selenol pair or two selenol moieties, respectively, at the 1,8-position of the naphthyl ring mediates the 5-deiodination of thyroid hormones and its endogenous metabolite iodothyronamines.[8] The chalcogen bonding between sulfur and selenium (**1**) or between two selenium atoms (**2**) at the *peri* positions of the naphthyl ring facilitates the halogen-bond-assisted cleavage of the C–I bond. In the present study, we show that iodothyronine sulfates can be deiodinated readily by synthetic deiodinase mimics. We also show for the first time that the strength of halogen bonding controls the regioselectivity and the rate of the deiodination of both thyroid hormones and their sulfate analogues.

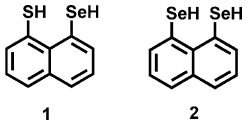

1 2

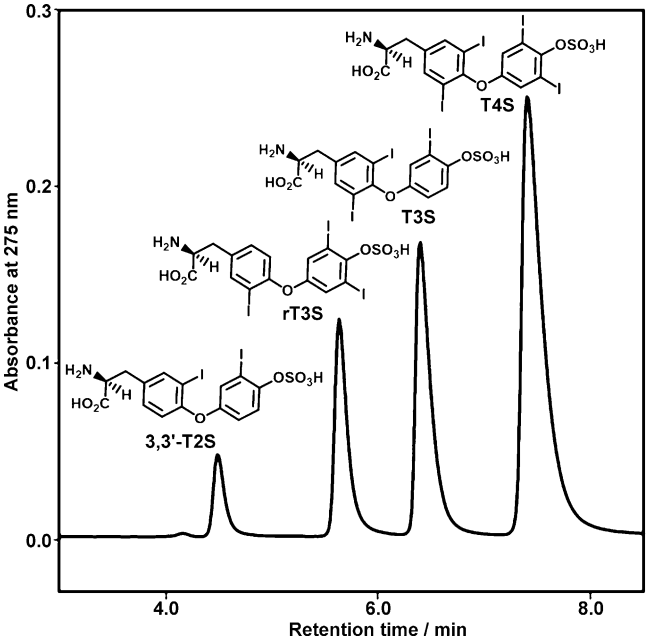

Figure 1. HPLC chromatogram obtained for the deiodination of **T4S** by **2**. The chemical structures of **T4S** and the deiodinated products are given on the respective peaks. Assay conditions: **T4S** (0.3 mM), **2** (0.6 mM), DTT (10 mM), $NaBH_4$ (15 mM), phosphate buffer (100 mM, pH 7.5), 37 °C.

Results and Discussion

The sulfated thyroid hormones (**T4S**, **T3S**, **rT3S**, **3,3′-T2S**) were synthesized from the corresponding thyroid hormones by using chlorosulfonic acid. The products of the deiodination reactions of thyroid hormones and their sulfate-conjugates by deiodinase mimics were monitored and analysed by HPLC. The deiodinated products were quantified by comparing the peak area with that of standard samples. As reported earlier in our laboratory,[8a,b] **1** and **2** mediate the deiodination of **T4** exclusively in the 5- ring to produce **rT3**. Interestingly, when **T4S** was treated with **1** or **2** in the presence of dithiothreitol (DTT) under identical experimental conditions, a decrease in the HPLC peak area for **T4S** was observed with three new peaks appearing at 6.4, 5.6 and 4.5 min (Figure 1). A comparison of the HPLC chromatograms obtained with that of the authentic samples of iodothyronine sulfates and mass spectral analyses indicate that **1** and **2** mediate both 5- and 5′-deiodinations of **T4S** to produce **rT3S**, **T3S** and **3,3′-T2S** (Figure 1). Therefore, sulfate conjugation of the phenolic hydroxyl group alters the regioselectivity of deiodination by deiodinase mimics. Although ID-1 catalyzes the 5-deiodination of **T4S** to produce **rT3S**, this enzyme does not catalyze the 5′-deiodination of **T4S**. These observations indicate that the synthetic compounds can mediate the 5′-deiodination of **T4S**, which is in contrast to the enzymatic reactions in which the 5′-deiodination of **T4** by ID-1 is blocked upon sulfation.

Interestingly, the sulfate conjugation not only changes the regioselectivity of deiodination, but also enhances the overall deiodination of **T4**. The initial rate for the overall deiodination of **T4S** by **1** was found to be almost 5.4 times higher than that for the 5-deiodination of **T4** (Figure 2). Similarly, **2** mediates a 7.6 times faster deiodination of **T4S** compared to **T4**. It should be noted that DTT does not mediate 5- or 5′-deiodination of **T4S** (Figure S1, Supporting Information).

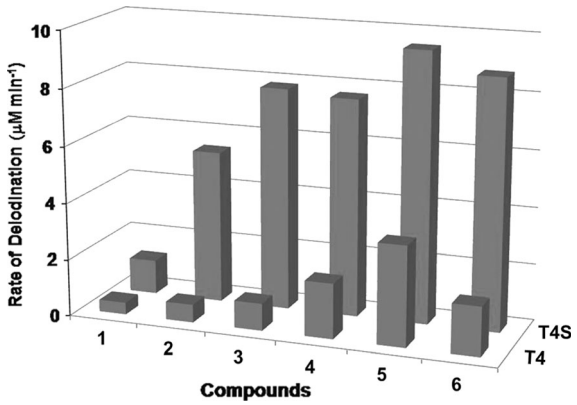

Figure 2. A comparison of the rate of deiodination of **T4** and **T4S** by **1**, **2** and **3**–**6**. The reactions were carried out in phosphate buffer (pH 7.5) at 37 °C. The final assay mixture contained 600 μM of **1**, **2** and **3**–**6**, 300 μM of **T4** or **T4S** and 10 mM of DTT.

T4S undergoes much faster 5′-deiodination than 5-deiodination by both compounds **1** and **2**. Interestingly, after one iodine atom has been removed from the tyrosyl or phenolic ring of **T4S**, the second iodine is removed from the other ring. Therefore, **rT3S** and **T3S** undergo only 5′- and 5-deiodination, respectively, by both **1** and **2** to produce **3,3′-T2S**. However, the 5′-deiodination of **rT3S** is 4–5 times faster than the 5-deio-

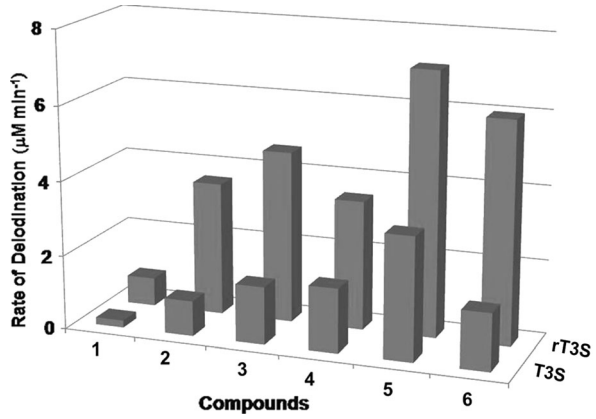

Figure 3. A comparison of the rate of deiodination of **T3S** and **rT3S** by compounds **1**, **2** and **3**–**6**. The reactions were carried out in phosphate buffer (pH 7.5) at 37 °C. The final assay mixture contained 600 μM of **1**, **2** and **3**–**6**, 300 μM of **T3S** or **rT3S** and 10 mM of DTT.

dination of **T3S** by **1** and **2** (Figure 3). These observations suggest that the removal of iodine from the 5′-position contributes significantly to the overall deiodinase activity observed with **T4S**. It should be noted that **rT3** does not undergo 5′-deiodination by **1** and **2** even at higher concentrations. However, as observed earlier for **3,3′-T2**, the corresponding sulfate analogue, **3,3′-T2S**, does not undergo further deiodination by **1** and **2**.

In agreement with the enzymatic deiodination, the deiodination of sulfated thyroid hormones by synthetic compounds is faster than that of the parent thyroid hormones. However, the mechanism by which sulfation enhances the deiodination of the thyroid hormones remains unknown. Also, the synthetic mimics of deiodinases lose their regioselectivity of deiodination upon sulfation of the thyroid hormones. To address these questions, we carried out detailed DFT calculations. Geometries were fully optimized in gas phase at the B3LYP level of theory by using the 6-311G** and 6-31+G* basis sets for iodine and other atoms, respectively. The electrostatic potential map indicates that the 5-iodine in **T4** have more positive potential (σ-hole)[9] than the 5′-iodine (Figure 4 and Table 1). Therefore, the iodine atoms at the 5-position of **T4** are expected to form stronger halogen bond with the selenium than the iodine at the 5′-position. On the other hand, sulfate conjugation of **T4** significantly increases the positive potential on the iodines at the 5′-position (Figure 2). In agreement with these observations, the natural bond orbital (NBO) analysis indicates that the 5-iodine in **T4** is more positively charged (0.207) relative to the 5′-iodine (0.174) (Table 1). In contrast, the 5′-iodine atom of **T4S** is more positively charged (0.239) than the 5-iodine (0.216). Therefore, 5′-iodine is expected to form much stronger halogen bond with selenium than the iodine at the 5-position. The 5′-iodine of **rT3S** has more positive charge than the 5-iodine, whereas the 5-iodine of **rT3** has more positive charge than the 5′-iodine. This may explain the reason for the facile 5′-deiodination of **rT3S** by **1** and **2**, and the inability of **rT3** to undergo deiodination under similar experimental conditions.

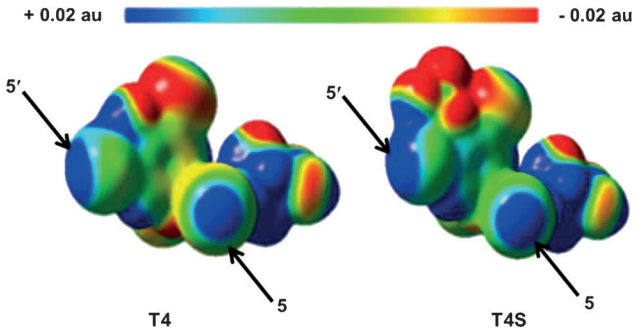

Figure 4. Electrostatic potential map of **T4** and **T4S**.

Table 1. NBO charge of iodine in different iodothyronines and their sulfate conjugates.[a]

Compound	5-Iodine	5′-Iodine	Compound	5-Iodine	5′-Iodine
T4	0.207	0.174	**T4S**	0.216	0.239
T3	0.206	0.192	**T3S**	0.213	0.219
rT3	0.192	0.178	**rT3S**	0.200	0.235
3,3′-T2	0.189	0.198	**3,3′-T2S**	0.200	0.184

[a] The structures were optimized at DFT level by using B3LYP/6-311G** for iodine and 6-31+G* for other atoms. The NBO analyses were performed with 6-311G** basis set for iodine and 6-311+G** for all other atoms and at the same level of theory.

A model selenol (MeSeH) was employed to understand the ability of the 5- and 5′-iodine atoms to form a halogen bond. As a selenol generally exists in its deprotonated selenolate form at a physiological pH of 7.4, it is more appropriate to use methyl selenolate ($MeSe^-$) in the theoretical calculations. However, owing to the difficulty in estimating the interaction involving the selenolate anion correctly, we used the selenium compound in its protonated form for the calculations. The halogen-bonded geometries of the thyroid hormones and their sulfated analogues were optimized by using the same level of theory and basis sets as discussed earlier. As expected, MeSeH forms halogen bonding with both the 5- and 5′-iodine atoms of **T4** and **T4S**. In all the geometries, the non-bonded distance between the selenium and iodine atom is shorter than the sum of their van der Waal radii (3.88 Å). However, the 5-iodine atom of **T4** forms a Se···I halogen bond that is a little shorter (3.741 Å) than the 5′-iodine (3.780 Å) (Figure 5). In contrast, the Se···I halogen bond formed by the 5- iodine atom of **T4S** (3.697 Å) is almost comparable to that formed by the 5′-iodine (3.727 Å). In all the halogen-bonded geometries formed by the 5- and 5′-iodine atoms of **T4** and **T4S**, the C–I···Se bond angle is ~180° whereas the I···Se–C bond angle is ~90°. These theoretically predicted geometries are quite similar to the observed Se···I halogen-bonded geometries obtained from single-crystal X-ray diffraction. It has been shown that tetramethylammonium selenocyanate (Me_4NSeCN) form quite strong Se···I halogen bonding with 1,2-diiodotetrafluorobenzene and 1,4-diiodotetrafluorobenzene.[10a] These halogen bonds have Se···I distances ranging from 3.394–3.552 Å, which indicates that these interactions are stronger than those observed in the present study. While the C–I···Se bond angles vary from 161.7 to 178.3°, the I···Se–C bond angles range from 80.9 to 111.7°. The halogen bonded adduct between 1,4-diiodotetrafluorobenzene and tri-

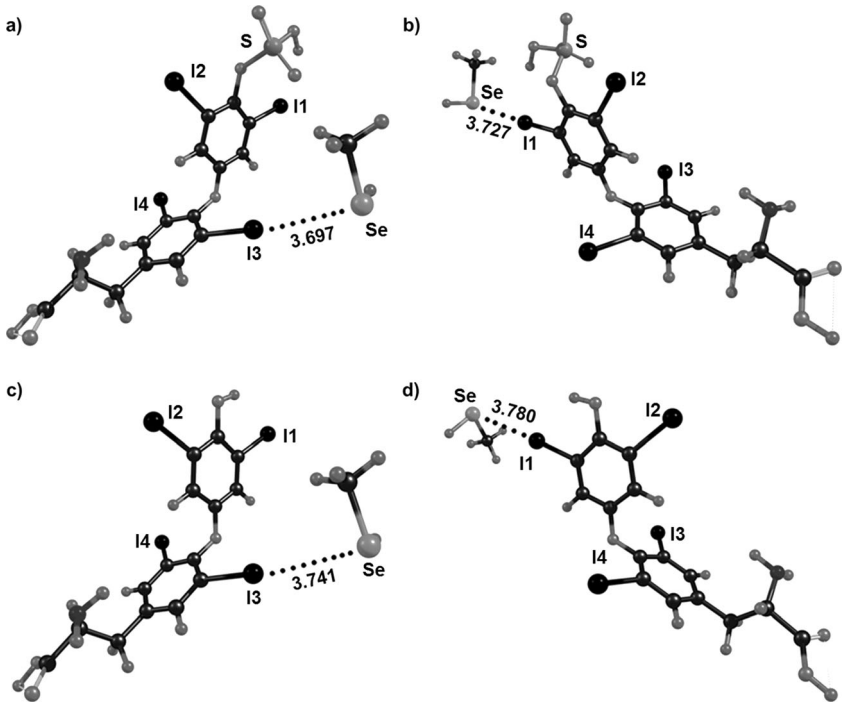

Figure 5. Comparison of the Se····I distances (Å) for the 5-ring and phenolic ring iodine atoms in the halogen-bonded adducts of **T4S** (a,b) and **T4** (c,d), respectively, with methyl selenol.

phenylphosphine selenide reveals Se···I distances of 3.394–3.639 Å, C–I···Se angles of 154.5–171.2° and I···Se–P angles of 89.6–112°.[10b] A similar adduct between 1,2-diiodotetrafluorobenzene and triphenylphosphine selenide also exhibits Se···I distances of 3.435 Å, C–I···Se angle of 170.9° and I···Se–P angle of 100.1°. The crystal packing of iododiisopropylphosphine selenide shows an Se···I halogen bonding with an Se···I distance of 3.642 Å.[10c] Similar types of compound iododi-*tert*-butylphosphine selenide shows two types of Se···I interactions with Se···I distances 3.69 and 3.844 Å.[10d]

To calculate the Se···I halogen-bonding interaction energies, NBO analysis was performed on the optimized halogen-bonded geometries using the same level of theory and basis sets as described earlier. The strength of halogen bonding may, at least partly, account for the differences in the reaction rates for the deiodination of thyroid hormones and their sulfate analogues. The Se···I interaction energy of the 5-iodine in **T4** with methyl selenol (4.18 kcal mol^{-1}) is higher than that of the 5′-iodine (3.83 kcal mol^{-1}; Table 2). Therefore, stronger halogen-bond energy may facilitate the selective removal of iodine from the 5-position. On the other hand, the 5′-iodine of the **T4S** forms a stronger halogen bond (5.19 kcal. mol^{-1}) with methyl selenol compared to the 5-iodine (4.98 kcal mol^{-1}). As both the 5- and 5′-iodine of **T4S** forms much stronger halogen bond with methyl selenol relative to **T4**, **T4S** may undergo both 5- and 5′-deiodination by **1** and **2**. The high interaction energies may also account for the faster deiodination of **T4S** compared to **T4**. After the removal of first iodine from the 5-position of **T4S**, the second iodine in the same ring of **rT3S** interacts much more weakly (4.36 kcal mol^{-1}) with methyl selenol. However, the 5′-iodine of **rT3S** forms even stronger halogen bonds (5.25 kcal. mol^{-1}) than the 5′-iodine of **T4S**. This may explain the selective phenolic ring deiodination of **rT3S** by **1** and **2**. However, these compounds do not deiodinate **rT3** even at the higher concentrations. This may be explained from the weak halogen-bond interaction energy (4.12 kcal mol^{-1}) between 5′-iodine of **rT3** and methyl selenol. The higher interaction energy for the 5-iodine (4.95 kcal. mol^{-1}) of **T3S** compared to the 5′-iodine (4.43 kcal. mol^{-1}) may explain the selective 5-ring deiodination of **T3S** by **1** and **2**. However, it is not clear why **3,3′-T2S**, with a reasonably strong Se···I interaction, does not undergo further deiodination.

Recently, we reported that the introduction of a basic amino group in the close proximity of one of the selenol moieties in **2** increases its reactivity (see compound **3**).[8b,c] As in the case of **T4** deiodination, **3** significantly enhances the deiodination of **T4S** and **rT3S** (Figure 2 and 3). Introduction of an additional amino group (**4**) or hydroxyl group (**5**) further enhances the deiodination. The deiodinase activity of **6**, which has a hydroxyl group instead of an

Table 2. The Se···I interaction energies for various iodothyronines and their sulfates with methyl selenolate.[a]

Compound	$E_{Se\cdots I}$ [kcal mol^{-1}]		Compound	$E_{Se\cdots I}$ [kcal mol^{-1}]	
	5-iodine	5′-iodine		5-iodine	5′-iodine
T4	4.18	3.83	**T4S**	4.98	5.19
T3	3.96	3.03	**T3S**	4.95	4.43
rT3	3.17	4.12	**rT3S**	4.36	5.25
3,3′-T2	3.20	3.61	**3,3′-T2S**	4.23	4.44

[a] The structures were optimized at DFT level by using B3LYP/6-311G** for iodine and 6-31+G* for other atoms. The NBO analyses were performed with 6-311G** basis set for iodine and 6-311+G** for all other atoms and at the same level of theory.

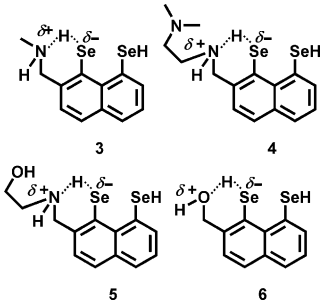

amino group, was found to be much higher than that of **3**; this indicates that substituents other than the amino group can also enhance the rate of deiodination. The thiols/selenols **4**–**6** required for the deiodinase assays were obtained by treating the corresponding dichalcogenides **10**–**12**. Compounds **10** and **11** were prepared by following the literature procedure (Scheme 2) and **12** was prepared by reducing **7** with $NaBH_4$.

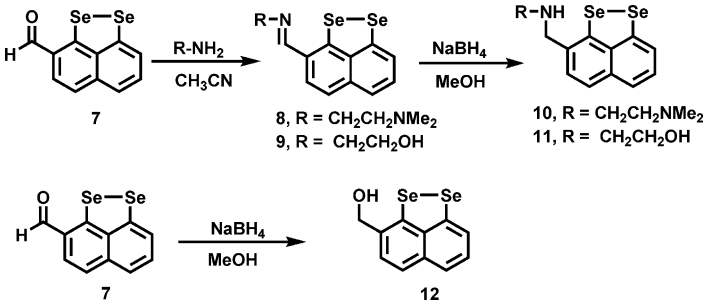

Scheme 2. Synthesis of dichalcogenides **10**–**12**.

Köhrle and others have reported that one of the histidine (His) residues may play an important role in the catalysis by forming an imidazolium–selenolate ion pair with the selenocysteine (Sec) residue at the active site of ID-1.[11] To understand the nature of selenol moieties in **4**–**6**, we have studied the ^{77}Se NMR spectral behaviour of these compounds. The ^{77}Se NMR spectra of compounds **4**, **5** and **6** showed that the signals for one of the selenol moieties are significantly shifted upfield ($\delta = 90$, 85 and 51 ppm, respectively) relative to the other selenol ($\delta = 217$, 216 and 208 ppm, respectively) (see Figures S7, S10 and S14, Supporting Information) in the same compound, which indicates that the *sec*-amino or hydroxyl groups form a hydrogen bond with the proximal selenol group as shown in the chemical structures of the compounds. The formation of a hydrogen bond between one of the selenols and the hydroxyl moieties in **6** is further supported by theoretical calculations. The SeH···O distance obtained from optimized geometry of **6** is 2.240 Å, which is within the range of moderately strong hydrogen-bonding distance. From the AIM analysis, a bond critical point was observed between SeH···O (Figure S23, Supporting Information). Formation of this kind of H-bond may ultimately lead to deprotonation of the selenol to produce selenolate. However, hydrogen bonding between a selenol and a nearby basic amine moiety should not interfere with the formation of Se···I halogen bonding because selenium forms a halogen bond through its lone pairs. Optimizing the geometry of iodobenzene with a model selenol, which is H-bonded to a nearby basic secondary amino group, leads to formation of moderately strong halogen-bonded adduct (Table S1, Supporting information).

The deprotonation of a selenol, to form a selenolate, is expected to form a stronger halogen bond with iodine. In our previous reports, we have shown that the initial rate of deiodination of **T4** by **2** increases with pH.[8b] This has been explained by deprotonation of the selenol at basic pH. Recently, Mobli and co-workers showed that the deprotonation of a Sec residue in peptides occurs at pH values as low as 3 and that Sec residues in different environments can exist completely in their selenolate forms at pH > 6.0.[12] However, the pK_a of the selenol in **2** could not be determined after several attempts mainly due to the difficulty in generating the diselenol from diselenide at acidic pH. When selenol is deprotonated to produce a selenolate, an upfield shift in ^{77}Se NMR spectra is expected. However, no such upfield shift in the ^{77}Se NMR spectra of **2** was observed between pH 7 and 11 (Figure S24, Supporting Information). These results indicate that the deprotonation of the selenol in **2** occurs below pH 7, which is consistent with the results reported by Mobli et al.

A recent crystal structure of the catalytic domain of mouse ID-3 indicates that Sec170 is responsible for the deiodination of thyroid hormones. Based on an Arg-T3-His clamp in **T3Rβ**, a model structure of ID-3 in complex with **T4** has been generated. His202, Arg275, Glu259 residues have been found to play an important role in the binding of **T4** to the ID-3 active site.[13] This binding mode placed the 5-iodine atom 3–4 Å away from the Sec residue. At this position, the selenol may form halogen-bonding contact with the σ-hole of iodine atom to elongate the C–I bond. The role of Se···I halogen bonding in the activation of C–I bond has been supported earlier by DFT studies.[14] After the iodine atom is removed as selenenyl iodide, the protonation of the 5-position occurs from the back side of the tyrosyl ring. The His219-Glu200-Ser167 triad along with Tyr197 and Thr169 residues have been shown to play an important role in proton transfer.[13]

In comparison to the Se···I halogen bond mediated 5-deiodination, tautomerisation of the enol form of **T4** (phenolic ring) to the corresponding keto form has been proposed to be crucial for the 5′-deiodination of **T4** by ID-1 (Scheme 3).[15] The 5-

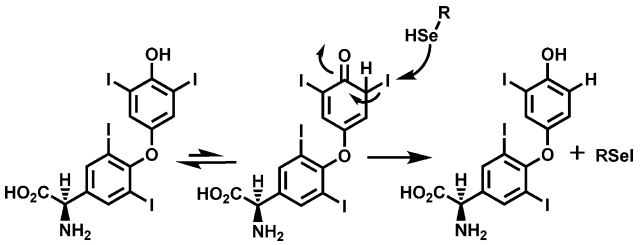

Scheme 3. Proposed mechanism of phenolic ring deiodination of **T4** through enol–keto tautomerism.

ring deiodination of **T4** by synthetic compounds involves cooperative halogen bonding and chalcogen bonding.[8c] A similar mechanism involving halogen-bond-assisted activation of the C–I bond is also possible for the removal of 5′-iodine. To understand the effect of the enol–keto tautomerism on the charge distribution of iodine, we carried out DFT calculations on both the keto tautomers of **T4**. It is known that the strength of halogen bond also depends on the hybridization of the carbon centre to which the halogen atom is attached. The halogen atom attached to an sp-hybridized carbon atom

forms the strongest halogen bond, followed by the ones that are attached to an sp^2 and sp^3 carbon atoms, respectively.[16] As the enol–keto tautomerism in **T4** leads to the formation of a partially sp^3-hybridized carbon atom (Figure 6), the phenolic ring iodines may become less reactive than the 5- ring iodines.

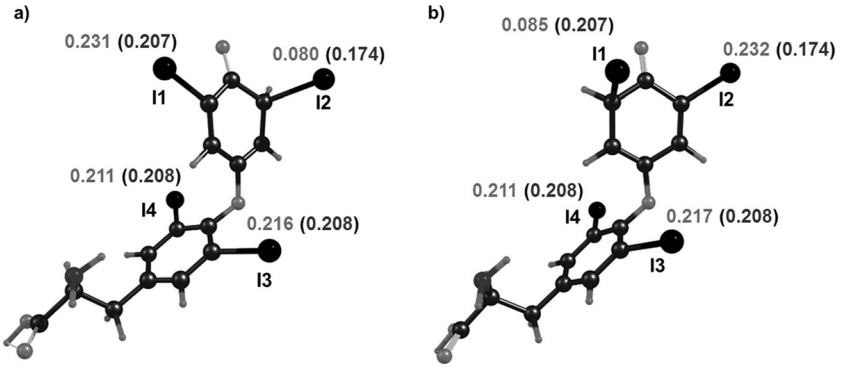

Figure 6. a) Electrostatic potential map of the keto form of **T4**. b) Effect of enol–keto tautomerism on the charge of iodine in **T4** (grey: charge in keto form; black: charge in enol form).

This is further supported by NBO analysis of both the enol and keto form of **T4**. The NBO analysis indicates that the positive charge of the iodine in the keto form (0.080 and 0.085) is considerably lower than the enol form (0.174 and 0.207). As a result, the average charge on the outer ring iodine atoms decreases from enol (0.191) to keto form (0.157). Therefore, the attack of selenol, as shown in Scheme 3, will be less favoured on the iodine in the keto form than in the enol form of **T4**. Blocking of the 4′-hydroxyl group by sulfate conjugation does not inhibit the phenolic ring deiodination by deiodinase enzymes. These observations indicate that the keto–enol tautomerism is not required to remove the phenolic ring iodine atoms of the thyroid hormones. However, under suitable conditions, phenolic ring iodine can also form a halogen bond with selenol and can undergo deiodination similar to the 5-iodine. Although **T4S** cannot undergo enol–keto tautomerism, the synthetic compounds are capable of mediating the phenolic ring deiodination. Also, the identical change in the activity of compounds **1**–**6** on moving from **T3S** to **rT3S** suggests that both the 5- and 5′-deiodinations occurs through a similar mechanism.

Conclusion

We showed that iodothyronine sulfates can be rapidly deiodinated by synthetic deiodinase mimics. In contrast to the selective 5-deiodination of **T4**, the synthetic compounds mediate both 5′- and 5-deiodinations of **T4S**. The overall rate of deiodination by the synthetic deiodinase mimics is increased upon sulfate conjugation. However, 5′-deiodination of **T4S** by ID-1 is completely blocked upon sulfation. For enzymatic deiodinase activity, besides the Se···I interaction, the binding affinity of the substrates to the active site of the enzyme also plays an important role. This study also reveals that the mechanisms by which the synthetic compounds perform the 5- and 5′-deiodinations are identical and an enol–keto tautomerism is probably not required for the 5′-deiodination of **T4** or **T4S**. It appears that halogen bonding is one of the crucial factors that control the regioselectivity of the deiodination of both thyroid hormones and their sulfate analogues. While the synthetic compounds reported in this paper function as ID-3 mimics with respect to thyroid hormones, their regioselectivity is altered when the sulfate analogues are used as substrates.

Experimental Section

Synthesis

Synthesis of T4S: L-Thyroxine (**T4**) (50 mg, 0.06 mmol) was dissolved in TFA (2 mL) and the solution was cooled to 0 °C. $ClSO_3H$ (100 μL) was added very slowly to this solution. A white precipitate appeared immediately. The reaction mixture was stirred at this temperature for 10 min. The resulting white suspension was poured to a beaker containing ice-cold water (5 mL). The resulting white suspension was centrifuged for 5 min at 8000 rpm and the solid obtained was washed thoroughly with water to remove excess TFA. The product (**T4S**) was purified by reverse-phase HPLC by using $MeOH/H_2O$ as the mobile phase. As this reaction produced a poor yield in higher molar scale, the reaction was repeated several times to obtain the desired amount of product. Yield: 40%; ^1H NMR (D_2O): $\delta = 2.56$–2.62 (dd, $J = 5.6$ Hz, 1H), 2.79–2.84 (dd, $J = 8$ Hz, 1H), 3.31–3.34 (m, 1H), 7.30 (s, 1H), 7.78 ppm (s, 1H); ^{13}C NMR (D_2O): $\delta = 36.5$, 57.7, 90.4, 90.5, 127.4, 140.8, 141.5, 148.2, 151.6, 153.9, 182.2 ppm; ESI-MS: *m/z*: calcd for $C_{15}H_{11}I_4NO_7S$: 857.65 $[M+H]^+$; found: 857.72.

Synthesis of T3S: 3,3′,5-Triiodothyronine (**T3**) (50 mg, 0.076 mmol) was dissolved in TFA (2 mL) and the resulting solution was cooled to 0 °C. $ClSO_3H$ (100 μL) was added very slowly to the solution. A white precipitate appeared immediately. The reaction mixture was stirred at this temperature for 10 min. The resulting white suspension was poured into ice-cold water (5 mL). The white suspension was centrifuged for 5 min at 8000 rpm. The white precipitate was washed thoroughly with water to remove excess TFA. Then it was purified by reverse-phase HPLC analysis using $MeOH/H_2O$ as the mobile phase. The reaction was repeated multiple times to get desired amount of product. Yield: 25%; ^1H NMR (D_2O): $\delta = 2.56$–2.62 (dd, 1H), 2.78–2.83 (dd, 1H), 3.32–3.35 (m,1H), 6.78–6.82 (dd, $J = 6.4$ Hz, 1H), 7.17 (s, 1H), 7.25 (d, $J = 8.6$, 1H), 7.68 ppm (s, 2H); ^{13}C NMR (D_2O): $\delta = 39.7$, 57.7, 90.7, 91.5, 117.2, 122.8, 126.1, 140.6, 141.4, 147.1, 151.9, 154.1, 182.1 ppm; ESI-MS: *m/z*: calcd for $C_{15}H_{12}I_3NO_7S$: 731.75 $[M+H]^+$; found: 731.79.

Synthesis of rT3S: 3,3′,5′-Triiodothyronine (**rT3**) (30 mg, 0.046 mmol) was dissolved in TFA (1 mL) and the resulting solution was cooled to 0 °C. $ClSO_3H$ (50 μL) was added very slowly to the solution. The resulting white suspension was poured into ice-cold water (3 mL). The white suspension was centrifuged for 5 min at 8000 rpm. The white precipitate was washed thoroughly with water to remove excess TFA. It was then purified by reverse-phase HPLC by using $MeOH/H_2O$ as the mobile phase. The reaction was

repeated multiple times to get desired amount of product. Yield: 21%; ^{1}H NMR (D_2O): δ = 2.59–2.64 (dd, 1H), 2.78–2.82 (dd, 1H), 3.31–3.34 (m, 1H), 6.65 (d, J = 8.4 Hz, 1H), 7.01–7.03 (dd, 1H), 7.31 (s, 2H), 7.64 ppm (1H); ^{13}C NMR (D_2O): δ = 40.1, 57.8, 89.3, 90.4, 121.4, 129.2, 131.7, 138.1, 140.9, 148.6, 153.6, 155.2, 182.5 ppm; ESI-MS: m/z: calcd for $C_{15}H_{12}I_3NO_7S$: 731.75 $[M+H]^+$; found: 731.76.

Synthesis of 3,3′-T2S: 3,3′-Diiodothyronine (**3,3′-T2**) (30 mg, 0.057 mmol) was dissolved in TFA (1 mL) and it was cooled to 0 °C. $ClSO_3H$ (50 μL) was added very slowly to the solution. The resulting white suspension was transferred into ice-cold water (3 mL). The white suspension was centrifuged for 5 min at 8000 rpm. The white precipitate was washed thoroughly with water to remove excess TFA. It was then purified by reverse-phase HPLC by using MeOH/H_2O as the mobile phase. The reaction was repeated multiple times to get desired amount of product. Yield: 16%; ^{1}H NMR (D_2O): δ = 2.98–3.04 (dd, 1H), 3.15–3.23 (dd, 1H), 3.96–3.99 (dd, 1H), 6.92–6.98 (m, 2H), 7.19 (d, J = 8.4 Hz, 1H), 7.31–7.34 (m, 2H), 7.77 ppm (s, 1H); ^{13}C NMR (D_2O): δ = 35.8, 56.3, 89.5, 91.4, 119.4, 121.0, 122.8, 128.5, 131.6, 134.1, 140.9, 147.7, 154.9, 155.2, 174.4 ppm; ESI-MS m/z: calcd for $C_{15}H_{13}I_2NO_7S$: 605.85 $[M+H]^+$; found: 605.80.

Synthesis of 10: *N*,*N*-Dimethylethylenediamine (1.76 g, 19.2 mmol) was added dropwise to a solution of naphthalene-1,8-diselenide-2-carboxaldehyde (**7**) (300 mg, 0.96 mmol) in dry acetonitrile (20 mL). The resulting reaction mixture was stirred at 60 °C for 12 h. The progress of the reaction was monitored by TLC analysis. The solvent was evaporated under reduced pressure after completion of the reaction. The resulting solid was dissolved in MeOH/$CHCl_3$ (5:1, 30 mL). $NaBH_4$ (726 mg, 19.2 mmol) was added to the above solution. The reaction mixture was stirred at room temperature for 3 h. The resulting red solution was poured into water (100 mL) and extracted with dichloromethane (40 mL). The dichloromethane extract was then dried and evaporated to give a red liquid, which was then purified by column chromatography using petroleum ether/ethyl acetate as eluent to give **10** as a red semisolid in 72% yield. ^{1}H NMR ($CDCl_3$): δ = 2.24 (s, 6H), 2.52 (t, J = 4.8 Hz, 2H), 2.68 (t, J = 6.0 Hz, 2H), 3.4 (s, 2H), 7.03 (d, J = 8.0 Hz, 1H), 7.18 (t, J = 7.6 Hz, 1H), 7.38 (d, J = 7.6 Hz, 1H), 7.45–7.49 ppm (m, 2H); ^{13}C NMR($CDCl_3$): δ = 45.9, 47.3, 53.6, 58.4, 123.0, 123.5, 124.8, 126.9, 127.5, 134.3, 136.8, 139.6, 140.6, 141.8 ppm; ^{77}Se NMR ($CDCl_3$): δ = 344, 475 ppm; ESI-MS: m/z: calcd for $C_{15}H_{18}N_2Se_2$: 386.98 $[M+H]^+$; found: 386.93.

Synthesis of 11: Ethanolamine (1.17 g, 19.2 mmol) was added dropwise to a solution of naphthalene-1,8-diselenide-2-carboxaldehyde (**7**) (300 mg, 0.96 mmol) in dry acetonitrile (20 mL). The resulting reaction mixture was stirred at 60 °C for 12 h. The progress of the reaction was monitored by TLC analysis. The solvent was evaporated under reduced pressure after completion of the reaction. The resulting solid was dissolved in MeOH/$CHCl_3$ (5:1, 30 mL). $NaBH_4$ (726 mg, 19.2 mmol) was added to the above solution. The reaction mixture was stirred at room temperature for 3 h. The resulting red solution was poured into water (100 mL) and extracted with dichloromethane (40 mL). The dichloromethane extract was then dried and evaporated to give a red liquid, which was then purified by column chromatography using petroleum ether/ethyl acetate as the eluent to give **11** as a red sticky oil in 75% yield. ^{1}H NMR ($CDCl_3$): δ = 2.81 (t, J = 4.8 Hz, 2H), 3.87 (t, J = 4.8 Hz, 2H), 4.00 (s, 2H), 7.02 (d, J = 8.1 Hz, 1H), 7.18 (t, J = 7.72 Hz, 1H), 7.40 (d, J = 8.0 Hz, 1H), 7.44 (d, J = 7.4 Hz, 1H), 7.49 ppm (d, J = 8.4 Hz, 1H); ^{13}C NMR($CDCl_3$): δ = 51.3, 53.7, 61.7, 123.1, 123.4, 124.9, 127.2, 127.6, 134.1, 136.9, 139.5, 140.4, 141.4 ppm; ^{77}Se NMR ($CDCl_3$): δ = 356, 455 ppm; ESI-MS: m/z: calcd for $C_{13}H_{13}NOSe_2$: 358.93 $[M]^+$; found: 358.92.

Synthesis of 12: Naphthalene-1,8-diselenide-2-carboxaldehyde (300 mg, 0.96 mmol) was dissolved in MeOH/$CHCl_3$ (5:1, 30 mL). $NaBH_4$ (726 mg, 19.2 mmol) was added to the above solution. The reaction mixture was stirred at room temperature for 2 h. The resulting brown solution was poured into water (100 mL) and extracted with dichloromethane (40 mL). The organic layer was washed with water. The dichloromethane extract was then dried and evaporated to give pure **12** as a deep-brown solid in 95% yield. ^{1}H NMR ($CDCl_3$): δ = 4.75 (s, 2H); 7.20–7.27 (m, 2H), 7.40 (d, J = 7.2 Hz, 1H), 7.46 (d, J = 8.0 Hz, 1H), 7.51 ppm (d, J = 7.2 Hz, 1H); ^{13}C NMR($CDCl_3$): δ = 66.3, 122.0, 123.7, 124.9, 127.2, 127.8, 133.9, 137.5, 138.8, 140.6, 140.8 ppm; ^{77}Se NMR ($CDCl_3$): δ = 406, 411 ppm; ESI-MS: calcd for $C_{11}H_8OSe_2$: 338.88 $[M+Na]^+$; found: 338.96.

Computational Studies

All calculations were performed by using the Gaussian 03 and 09 suites of quantum chemical programs.[17] The hybrid B3LYP exchange correlation functional was employed to predict the minimum energy molecular geometries of the compounds.[18] Geometries were fully optimized in the gas phase at the B3LYP level of theory by using the 6-31 + G* basis set for all atoms except iodine, for which it does not exist. Therefore, the 6-311 G** basis set was used for iodine. Frequency calculations were performed on each optimized structure using the same basis set to ensure that it was a minimum on the potential-energy surface. NBO calculations[19] were performed with the 6-311 G** basis set for iodine and 6-311 + G** for all other atoms and the same level of theory. Electrostatic potential maps of thyroid hormones were mapped on the surface of molecular electron density 0.01 au by using Gauss View 5.0 software.

Acknowledgements

This study was supported by the Science and Engineering Research Board (SERB), Department of Science and Technology (DST) and Department of Biotechnology (DBT), New Delhi. D.M. and S.M. thank the Indian Institute of Science for a research fellowship.

Keywords: enzyme mimics · halogen bonding · iodothyronine deiodinase · sulfate conjugatation · thyroid hormones

[1] a) D. Behne, A. Kyriakopoulos, H. Meinhold, J. Köhrle, *Biochem. Biophys. Res. Commun.* **1990**, *173*, 1143–1149; b) J. L. Leonard, T. J. Visser in *Biochemistry of Deiodination in Thyroid Hormone Metabolism* (Ed.: G. Hennemann), Marcel Dekker, New York, **1986**, p. 189; c) M. J. Berry, L. Banu, P. R. Larsen, *Nature* **1991**, *349*, 438–440; d) P. R. Larsen, M. J. Berry, *Annu. Rev. Nutr.* **1995**, *15*, 323; e) J. L. Leonard, J. Köhrle in *Intracellular Pathways of Iodothyronine Metabolism in The Thyroid* (Eds.: L. E. Braverman, R. D. Utiger), Lippincott-Raven, Philadelphia, **1996**, p. 144; f) D. L. St. Germain, V. A. Galton, *Thyroid* **1997**, *7*, 655–668.

[2] a) A. C. Bianco, D. Salvatore, B. Gereben, M. J. Berry, P. R. Larsen, *Endocr. Rev.* **2002**, *23*, 38–89; b) J. Köhrle, *Methods Enzymol.* **2002**, *347*, 125–167; c) G. G. J. M. Kuiper, M. H. A. Kester, R. P. Peeters, T. J. Visser, *Thyroid* **2005**, *15*, 787–798.

[3] a) B. A. Rikke, A. K. Roy, *Biochim. Biophys. Acta* **1996**, *1307*, 331–338; b) C. N. Falany, *FASEB J.* **1997**, *11*, 1–2.

[4] M. Michio, H. Hiroshi, *Int. J. Biochem.* **1994**, *26*, 1237–1247.

[5] a) R. M. Weinshilboum, D. M. Otterness, I. A. Aksoy, T. C. Wood, C. Her, R. B. Raftogianis, *FASEB J.* **1997**, *11*, 3–14; b) C. N. Falany, X. Xie, J. Wang, J. Ferrer, J. L. Falany, *Biochem. J.* **2000**, *346*, 857–864; c) M. H. Kester, E. Kaptein, T. J. Roest, C. H. van Dijk, D. Tibboel, W. Meinl, H.

Glatt, M. W. Coughtrie, T. J. J. Visser, *Clin. Endocrinol. Metab.* **1999**, *84*, 1357 – 1364; d) M. H. Kester, C. H. van Dijk, D. Tibboel, A. M. Hood, N. J. Rose, W. Meinl, U. Pabel, H. Glatt, C. N. Falany, M. W. Coughtrie, T. J. J. Visser, *Clin. Endocrinol. Metab.* **1999**, *84*, 2577 – 2586.

[6] a) R. D. Sekura, K. Sato, H. J. Cahnmann, J. Robbins, W. B. Jakoby, *Endocrinology* **1981**, *108*, 454 – 456; b) W. F. Young, C. A. Gorman, R. M. Weinshilboum, *Endocrinology* **1988**, *122*, 1816 – 1824; c) D. W. Gong, N. Murayama, Y. Yamazoe, R. Kato, *J. Biochem.* **1992**, *112*, 112 – 116; d) R. E. Hurd, F. Santini, P. Naim, B. Lee, I. J. Chopra, *Clin. Res.* **1993**, *41*, A62; e) T. J. Visser, J. A. Mol, M. H. Otten, *Endocrinology* **1983**, *112*, 1547 – 1549; f) M. H. Otten, J. A. Mol, T. J. Visser, *Science* **1983**, *221*, 81 – 83; g) M. Rutgers, F. A. Heusdens, T. J. Visser, *Endocrinology* **1991**, *129*, 1375 – 1381; h) F. Santini, R. E. Hurd, I. J. Chopra, *Endocrinology* **1992**, *131*, 1689 – 1694; i) F. Santini, I. J. Chopra, S. Y. Wu, D. H. Solomon, G. N. C. Teco, *Pediatr. Res.* **1992**, *31*, 541 – 544; j) S. J. E. Rooda, E. Kaptein, M. A. C. van Loon, T. J. Visser, *J. Immunoassay* **1988**, *9*, 125 – 134.

[7] a) J. A. Mol, T. J. Visser, *Endocrinology* **1985**, *117*, 8 – 12; b) J. A. Mol, T. J. Visser, *Endocrinology* **1985**, *117*, 1 – 7.

[8] a) D. Manna, G. Mugesh, *Angew. Chem.* **2010**, *122*, 9432 – 9435; *Angew. Chem. Int. Ed.* **2010**, *49*, 9246 – 9249; b) D. Manna, G. Mugesh, *J. Am. Chem. Soc.* **2011**, *133*, 9980 – 9983; c) D. Manna, G. Mugesh, *J. Am. Chem. Soc.* **2012**, *134*, 4269 – 4279; d) S. Mondal, G. Mugesh, *Chem. Eur. J.* **2014**, *20*, 11120 – 11128.

[9] a) P. Politzer, P. Lane, M. C. Concha, Y. Ma, J. S. Murray, *J. Mol. Model.* **2007**, *13*, 305 – 311; b) T. Clark, M. Hennemann, J. S. Murray, P. Politzer, *J. Mol. Model.* **2007**, *13*, 291 – 296.

[10] a) J. Viger-Gravel, I. Korobkov, D. L. Bryce, *Cryst. Growth Des.* **2011**, *11*, 4984 – 4995; b) H. D. Arman, E. R. Rafferty, C. A. Bayse, W. T. Pennington, *Cryst. Growth Des.* **2012**, *12*, 4315 – 4323; c) C. G. Daniliuc, C. G. Hrib, P. G. Jones, W.-W. du Mont, *Cryst. Growth Des.* **2012**, *12*, 185 – 188; d) J. Jeske, W.-W. du Mont, P. G. Jones, *Chem. Eur. J.* **1999**, *5*, 385 – 389.

[11] a) J. Köhrle, R. D. Hesch, *Horm. Metab. Res. Suppl.* **1984**, *14*, 42 – 55; b) M. J. Berry, *J. Biol. Chem.* **1992**, *267*, 18055 – 18059; c) J. A. Mol, R. Docter, G. Hennemann, T. J. Visser, *Biochem. Biophys. Res. Commun.* **1984**, *120*, 28 – 36.

[12] M. Mobli, D. Morgenstern, G. F. King, P. F. Alewood, M. Muttenthaler, *Angew. Chem.* **2011**, *123*, 12158 – 12161; *Angew. Chem. Int. Ed.* **2011**, *50*, 11952 – 11955.

[13] U. Schweizer, C. Schlicker, D. Braun, J. Köhrle, C. Steegborn, *Proc. Natl. Acad. Sci. USA* **2014**, *111*, 10526 – 10531.

[14] C. A. Bayse, E. R. Rafferty, *Inorg. Chem.* **2010**, *49*, 5365 – 5367.

[15] a) C. Beck, S. B. Jensen, J. Reglinski, *Bioorg. Med. Chem. Lett.* **1994**, *4*, 1353 – 1356; b) A. A. Vasil'ev, L. Engman, *J. Org. Chem.* **1998**, *63*, 3911 – 3917; c) K. Goto, D. Sonoda, K. Shimada, S. Sase, T. Kawashima, *Angew. Chem.* **2010**, *122*, 555 – 557; *Angew. Chem. Int. Ed.* **2010**, *49*, 545 – 547.

[16] a) P. Metrangolo, H. Neukirch, T. Pilati, G. Resnati, *Acc. Chem. Res.* **2005**, *38*, 386 – 395; b) E. Parisini, P. Metrangolo, T. Pilati, G. Resnati, G. Terraneo, *Chem. Soc. Rev.* **2011**, *40*, 2267 – 2278.

[17] a) Gaussian 03, Revision C.02, M. J. Frisch, G. W. Trucks, H. B. Schlegel, G. E. Scuseria, M. A. Robb, J. R. Cheeseman, J. A. Jr. Montgomery, T. Vreven, K. N. Kudin, J. C. Burant, J. M. Millam, S. S. Iyengar, J. Tomasi, V. Barone, B. Mennucci, M. Cossi, G. Scalmani, N. Rega, G. A. Petersson, H. Nakatsuji, M. Hada, M. Ehara, K. Toyota, R. Fukuda, J. Hasegawa, M. Ishida, T. Nakajima, Y. Honda, O. Kitao, H. Nakai, M. Klene, X. Li, J. E. Knox, H. P. Hratchian, J. B. Cross, C. Adamo, J. Jaramillo, R. Gomperts, R. E. Stratmann, O. Yazyev, A. J. Austin, R. Cammi, C. Pomelli, J. W. Ochterski, P. Y. Ayala, K. Morokuma, G. A. Voth, P. Salvador, J. J. Dannenberg, V. G. Zakrzewski, S. Dapprich, A. D. Daniels, M. C. Strain, O. Farkas, D. K. Malick, A. D. Rabuck, K. Raghavachari, J. B. Foresman, J. V. Ortiz, Q. Cui, A. G. Baboul, S. Clifford, J. Cioslowski, B. B. Stefanov, G. Liu, A. Liashenko, P. Piskorz, I. Komaromi, R. L. Martin, D. J. Fox, T. Keith, M. A. Al-Laham, C. Y. Peng, A. Nanayakkara, M. Challacombe, P. M. W. Gill, B. Johnson, W. Chen, M. W. Wong, C. Gonzalez, J. A. Pople, Gaussian, Inc., Wallingford CT, **2004**; b) Gaussian 09, Revision A.1, M. J. Frisch, G. W. Trucks, H. B. Schlegel, G. E. Scuseria, M. A. Robb, J. R. Cheeseman, G. Scalmani, V. Barone, B. Mennucci, G. A. Petersson, H. Nakatsuji, M. Caricato, X. Li, H. P. Hratchian, A. F. Izmaylov, J. Bloino, G. Zheng, J. L. Sonnenberg, M. Hada, M. Ehara, K. Toyota, R. Fukuda, J. Hasegawa, M. Ishida, T. Nakajima, Y. Honda, O. Kitao, H. Nakai, T. Vreven, J. A. Jr. Montgomery, J. E. Peralta, F. Ogliaro, M. Bearpark, J. J. Heyd, E. Brothers, K. N. Kudin, V. N. Staroverov, R. Kobayashi, J. Normand, K. Raghavachari, A. Rendell, J. C. Burant, S. S. Iyengar, J. Tomasi, M. Cossi, N. Rega, N. J. Millam, M. Klene, J. E. Knox, J. B. Cross, V. Bakken, C. Adamo, J. Jaramillo, R. Gomperts, R. E. Stratmann, O. Yazyev, A. J. Austin, R. Cammi, C. Pomelli, J. W. Ochterski, R. L. Martin, K. Morokuma, V. G. Zakrzewski, G. A. Voth, P. Salvador, J. J. Dannenberg, S. Dapprich, A. D. Daniels, Ö. Farkas, J. B. Foresman, J. V. Ortiz, J. Cioslowski, D. J. Fox, Gaussian, Inc., Wallingford CT, **2009**.

[18] a) A. D. Becke, *J. Chem. Phys.* **1993**, *98*, 5648 – 5652; b) C. Lee, W. Yang, R. G. Parr, *Phys. Rev. B* **1988**, *37*, 785 – 789.

[19] a) A. E. Reed, L. A. Curtiss, F. Weinhold, *Chem. Rev.* **1988**, *88*, 899 – 926; b) E. D. Glendening, J. E. Reed, J. E. Carpenter, F. Weinhold, NBO Program 3.1; Madison, WI, **1988**.

Received: September 28, 2014
Published online on December 8, 2014